Journal of
Manufacturing and Materials Processing

MDPI

Article

Identification of the Mechanism Resulting in Regions of Degraded Toughness in A508 Grade 4N Manufactured Using Powder Metallurgy–Hot Isostatic Pressing

Colin D. Ridgeway *, Terrance Nolan and Joeseph M. Pyle

Naval Nuclear Laboratory, Knolls Atomic Power Laboratory, Niskayuna, NY 12309, USA; joseph.pyle@unnpp.gov (J.M.P.)
* Correspondence: colin.ridgeway@unnpp.gov

Abstract: Powder metallurgy–hot isostatic pressing (PM-HIP) is a form of advanced manufacturing that offers the ability to produce near-net shape components that are otherwise not achievable via conventional forging or wrought manufacturing. Accessing the design space of PM-HIP is dependent upon the ability to achieve uniform or known properties in finalized components, which has resulted in a number of programs aimed at identifying properties achievable via PM-HIP manufacturing. One result of these programs has been the consistent observation of a variation in toughness observed for the low-alloy steel ASTM A508 Grades 3 and 4N. While observed, the degree of variability and the mechanism resulting in the variability have not yet been fully defined. Thus, a systematic approach to evaluate the variation observed in impact toughness in PM-HIP ASTM A508 Grade 4N was proposed to elucidate the responsible metallurgical mechanism. Four unique billets manufactured from two heats of powder with different particle size distributions (PSDs) were fabricated and tested for impact toughness and tensile properties. The degradation in impact toughness was confirmed to be location-specific where the near-can region of all billets had reduced impact toughness relative to the interior of each billet. The mechanism driving the location-specific property development was identified to be mobile oxygen that follows the thermal gradient that develops during the HIP cycle and leads to a redistribution of mobile oxygen where oxygen is concentrated ~1" inboard of the original canister/billet interface. Redistributed oxygen then forms stable oxides along coincident prior particle and prior austenite grain boundaries, effectively reducing the impact toughness. With the mechanism now addressed, necessary actions can be taken to mitigate the effect of the oxygen redistribution, allowing for use in PM-HIP A508 Grade 4N in commercial industry.

Keywords: powder metallurgy–hot isostatic pressing (PM-HIP); submarine industrial base (SIB); nuclear powder; A508 grade 4N; oxygen migration

Citation: Ridgeway, C.D.; Nolan, T.; Pyle, J.M. Identification of the Mechanism Resulting in Regions of Degraded Toughness in A508 Grade 4N Manufactured Using Powder Metallurgy–Hot Isostatic Pressing. *J. Manuf. Mater. Process.* **2024**, *8*, 132. https://doi.org/10.3390/jmmp8040132

Academic Editor: Prashanth Konda Gokuldoss

Received: 30 April 2024
Revised: 21 June 2024
Accepted: 21 June 2024
Published: 26 June 2024

1. Introduction

Advanced manufacturing in the form of PM-HIP has become increasingly popular due to increased demand in the aerospace, military, nuclear, and power industries. PM-HIP offers the ability to fabricate fully densified near-net shape components by employing the combination of a sheet metal capsule filled with metal powder and hot isostatic pressing (HIP) to realize complex geometries that are otherwise not achievable via traditional wrought manufacturing [1]. Utilizing the PM-HIP process also offers the opportunity to reduce component fabrication lead times, reduce the material required to produce large scale components, and eliminate welds by combining multiple complex geometrical designs into single components [2]. The culmination of each of these variables leads to an overall cheaper product that can be delivered to the end consumer at a faster rate.

The appeal of the PM-HIP process is only heightened by the increasingly long lead times currently being experienced to obtain large-scale components for military and nuclear applications. The Electric Power Research Institute (EPRI) completed a study in 2016 that

concluded that the United States has experienced a steady decline in the capacity of domestic forge houses and indicated that a number of the world's largest forge houses now reside in other countries including Japan, Italy, and South Korea [2]. The recently issued US Department of Defense National Defense Industrial Strategy (NDIS) highlights the need for the United States to invest in and develop more dynamic production and capabilities [3]. Specifically, investments are being directed to the United States' Submarine Industrial Base (SIB) to increase production rates and submarine availability through initiatives in supplier development, shipbuilder and supplier infrastructure, workforce development, technology advancements, government oversight, and strategic sourcing [4]. This additional capability is necessary to support projected shipbuilding plans [5–7] that will require a 250% increase in construction capacity (tonnage) relative to recent production rates.

A key material of interest for evaluation via PM-HIP is the pressure vessel steel ASTM A508 due to its prevalent use in the nuclear industry and power generation systems. Both EPRI and Rolls Royce have explored the properties of ASTM A508 Grade 3 and Grade 4N, respectively. EPRI's work [2,8] on PM-HIP A508 Grade 3 has largely consisted of analyses of air-melted powder and has shown that Charpy impact toughness in excess of 110 ft-lbs is achievable for laboratory-scale sized billets (6 × 6 × 6 in.). However, EPRI also observed a large degree of variability in the impact toughness of A508 Grade 3 for both laboratory and large-scale demonstration components. In one such demonstration component, EPRI noted a range in impact toughness varying from 48 to 118 ft-lbs [8]. Such a large variation is not suitable for nuclear systems and EPRI is exploring pathways to improve the consistency in impact toughness.

Alternatively, Rolls Royce has focused on the assessment of A508 Grade 4N sourced from both air-melt and vacuum-melted powders [9–11]. Despite the refined chemistry (Table 1), Rolls Royce has experienced similar issues in regard to variation with impact toughness. In an extreme case, Rolls Royce has cited one batch of powder in the consolidated condition that was only able to achieve 21% of the forged equivalent impact toughness at room temperature, with other batches measuring near 66% of the forged equivalent [11]. The latest work from Rolls Royce [11] has shown that by utilizing an oxide stripping process, the impact toughness can be improved and may be potentially satisfactory for design in nuclear systems. The trend for impact toughness variability for A508 Grade 4N was also observed by Ridgeway et al. [7], who identified that the impact toughness variation had a location-specific correlation. Ridgeway et al. observed that specimens extracted near the original powder/canister interface were much lower in impact toughness relative to specimens extracted from the interior of the original cross section. Despite the consistent observation of the variable/degraded impact toughness, there has yet to be a mechanism proposed that accurately describes the degradation in impact toughness. Thus, the discussion herein focuses on the characterization of the mechanical properties, specifically the impact toughness, within PM-HIP A508 Grade 4N material and the development of the metallurgical mechanism responsible for the variations observed. Once the metallurgical mechanism resulting in the degraded toughness is defined, efforts can be completed to mitigate this effect and allow for usage of PM-HIP A508 Grade 4N within commercial industries.

Table 1. General chemistry of various grades of ASTM A508 low-alloy steel.

Material	Fe	C	Mn	P	S	Si	Ni	Cr	Mo	V	Ti	O
Grade 3	Bal.	0.25	1.20–1.50	0.025	0.025	0.40	0.40–1.00	0.25	0.45–0.60	0.05	0.015	–
Grade 4N	Bal	0.23	0.20–040	0.020	0.020	0.40	2.8–3.9	0.25	0.40–0.60	0.03	0.015	–

Note: All values are a maximum.

2. Materials and Methods

A total of four (4) billets were fabricated and analyzed to explore the variation in impact toughness properties described above. The billets were produced from multiple heats of powder with different PSDs to ensure that the variation in properties exhibited

in prior research was still present across various powder heats with different PSDs and processing conditions, noted in Table 2. Each of the billets evaluated in this study was given a randomized ID, with the billet ID (NC9/ND2/ND6/ND8) indicating no significance. Confirmation of the variation in properties at various location in the billets under various processing conditions will also confirm that the degradation in near-can impact toughness cannot be resolved via standard pre-HIP processing. The methods used for material processing are listed below.

Table 2. Billet fabrication details.

Billet ID	Powder Vendor	Powder PSD (μm)	Powder Oxygen (ppm)	Nominal Billet Size	Outgas Temperature	HIP Temp./Pressure	HIP Time
NC9	A (Heat 1)	0–500	166	8″ × 8″ × 18″	21 °C	1212 °C/100 MPa	4 h
ND2	A (Heat 1)	0–500	166	8″ × 8″ × 18″	260 °C	1212 °C/100 MPa	4 h
ND6	A (Heat 2)	53–500	97	8″ × 8″ × 18″	21 °C	1212 °C/100 MPa	4 h
ND8	A (Heat 2)	53–500	97	8″ × 8″ × 18″	260 °C	1212 °C/100 MPa	4 h

2.1. Powder Sourcing and Billet Fabrication

All billets analyzed were fabricated using vacuum-melted powder and utilized two PSDs. The first heat of powder was full-cut powder with a PSD of 0–500 μm, while the second heat removed the fine particles (<53 μm), effectively lowering the oxygen content. Each of the powders was placed into welded mild steel canisters, where they were then vacuum-outgassed before HIP consolidation using the parameters detailed in Table 2. All billets were fabricated to have post-HIP cross sectional dimensions of 8″ × 8″, with a minimum height of 16″. The cross-sectional size was chosen so that sufficient material was available to delineate the difference in properties from the near-can regions and billet interior. For each of the powders examined, the oxygen content was elevated, ranging from 97 to 166 ppm, with respect to standard expected values commensurate with modern vacuum-degassed steel production. However, the ASTM chemistry specification A508 Grade 4N does not establish an explicit minimum oxygen content, and elevated oxygen levels are expected in all powder products and is the result of the atomization process. The variation in oxygen content is a result of the two different PSD ranges evaluated, where full-cut powder (0–500 μm) is associated with increased oxygen content owing to the increased overall surface area of powder relative to the powder with fine particles removed. An analysis of HIP-consolidated material fabricated from varying PSDs allowed for an examination of the effect of the initial powder content on the final impact toughness of PM-HIP-consolidated A508 Grade 4N.

2.2. Post-HIP Heat Treatment

ASTM A508 is a quench and temper steel and requires heat treatment to be used in its final form. Following the HIP consolidation, four 4 in. thick cross sections were removed from each of the billets with the end crops (~1 in.) discarded. The 4 in. thick cross sections were then cut in half to reveal eight sub-sections nominally measuring 4 × 4 × 8 in., as shown in Figure 1c. Billet sub-sections (4 × 4 × 8 in.) were heat treated via an austenization (855 °C–4 h) followed by water quench and then a temper (652 °C–10 h). During all heat treatments, the mild-steel canister was left intact so that the original interface could be tracked. For the remainder of the analysis, only a single sub-section (4 × 4 × 8 in.) from the bottom right corner, as shown in Figure 1c, from each billet was used, and all other sub-sections were reserved for future studies.

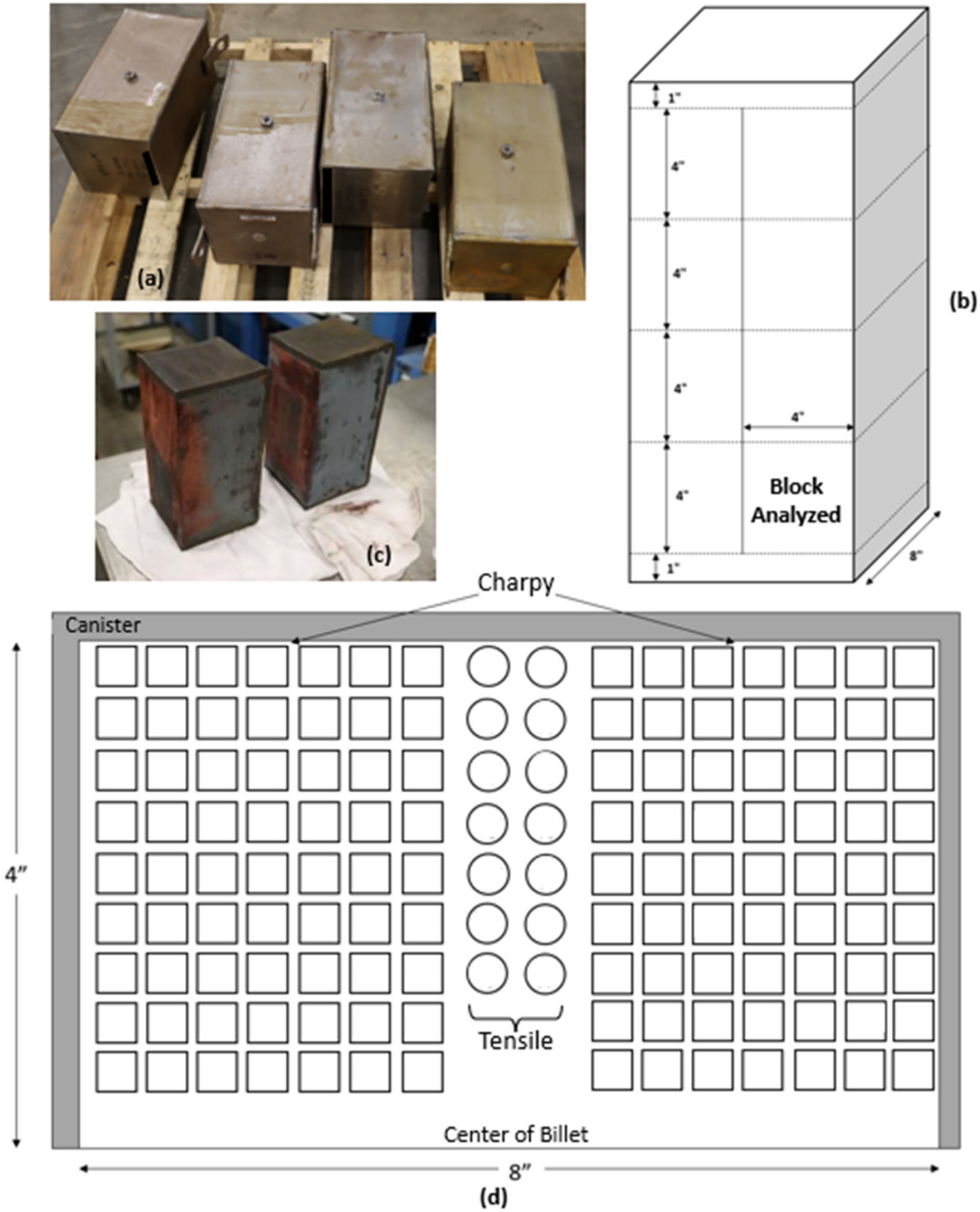

Figure 1. (**a**) As-HIP'ed A508 Grade 4N billets with (**b**) a 3D sketch showing billet sub-section extraction locations. (**c**) The $4'' \times 4'' \times 8''$ sub-sections following austenization, water quench, and temper. (**d**) Specimen extraction layout for NC9/ND2/ND6/ND8 with squares representing Charpy specimens and circles representing tensile specimens. The specimen extraction layout provides a visualization of each Charpy specimen distance/position from the canister and can be correlated to Figure 2.

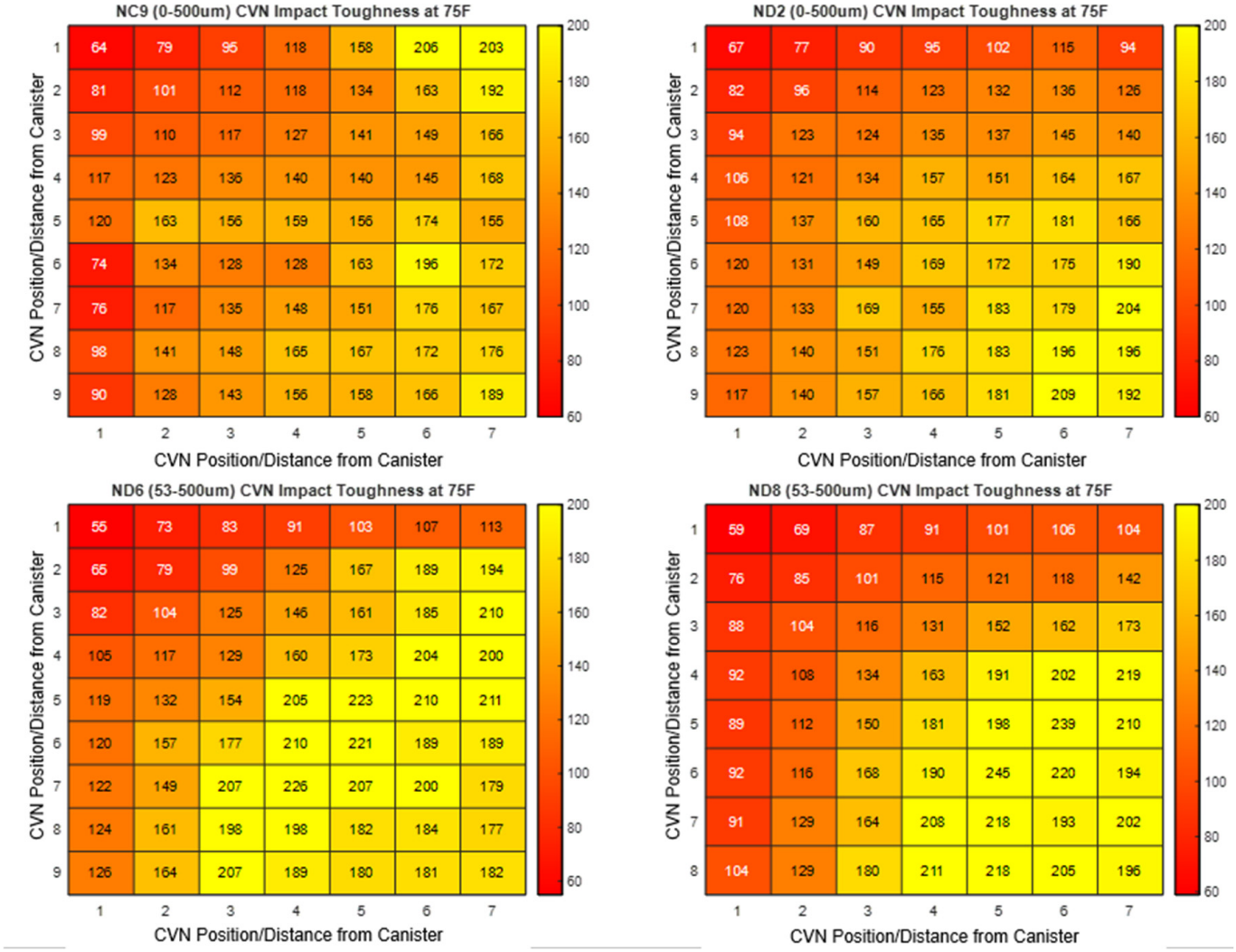

Figure 2. Charpy impact toughness heat maps collected at 24 °C for C9, ND2, ND6, and ND8. All data displayed in ft-lbs of toughness as a function of specimen position/distance from the canister. The x/y-axis is the position/distance of each Charpy position correlating to a distance (defined as 0.4 in. multiplied by specimen position), as detailed in Section 2.2. The canister edge was located on the top and left-hand side for all heat maps.

2.3. Specimen Extraction Locations and Testing

In order to fully characterize the degradation in impact toughness at the near-can region in PM-HIP A508 Grade 4N, an extensive number of Charpy specimens were required. In total, 126 Charpy specimens were extracted from each of the billets, which were broken down into two sets of 63 Charpy specimens, as shown in Figure 1d. Each set comprised 9 rows of specimens, where the corner specimen in the Charpy matrix was located as close as possible to the corner of the billet without containing any canister material. All specimens were extracted via EDM and then finally machined to the ASTM E23 standard Charpy V-Notch specimen size (0.393 × 0.393 in. cross section and 2.165 in. length). EDM was chosen to ensure that each Charpy specimen was extracted as close as possible to its nearest neighbor. Including blade kerf, it was judged that the total width of a single Charpy was approximately 0.40″, which was used as the unit of measure for the spacing of all Charpy specimens, as discussed in the subsequent section. Thus, in a given column, the Charpy specimens located closest to the canister would be extracted between 0 and 0.4 in. from the canister and the second Charpy specimen would be 0.4–0.8 in from the canister, with this spacing repeated for all specimens. In order to eliminate the test temperature as

a potential variable, each set of 63 specimens from each billet was tested per ASTM E23 at a single temperature to fully characterize the impact toughness response. One set of 63 specimens from each billet (left-hand side per Figure 1b) was tested at the upper shelf (24 °C). The remaining 63 specimens from each billet (right-hand side per Figure 1d) were held in reserve for future testing.

Tensile specimens were extracted similar to the Charpy specimens with the EDM tensile blanks removed from the sub-section and then machined to their final size. All tensile specimens were machined to the ASTM E8 standard size specimen for cylindrical specimens with a gauge length four times the diameter (2 in. gauge and 0.5 in. diameter). The tensile specimen extraction locations are also detailed in Figure 1d, with the specimens extracted from the center of the billet in 7 rows of 2 specimens to identify if there was any variation in the tensile properties as a function of specimen distance from the canister. All tensile testing was completed at 24 °C per ASTM E8 procedures.

3. Results and Discussion

3.1. Charpy Impact Toughness

Charpy impact toughness was measured at a single temperature (24 °C) for each billet to assess the upper shelf (24 °C) impact energy of PM-HIP A508 Grade 4N. The impact toughness performance was judged against an arbitrary upper shelf target of 100 ft-lbs at 24 °C.

An analysis of the resulting Charpy impact toughness for each billet in Figure 2 confirms the trend of location-dependent impact toughness. In all cases, the specimens located closest to the original canister/billet interface (left-hand and top side of all plots in Figure 2) had the lowest impact toughness. As the distance from the canister increases, the impact toughness is seen to rise until it stabilizes or plateaus near 2″ inboard of the canister wall. The impact toughness ranged from as low as 55 ft-lbs (ND6) at the near-can corner, all the way to 239 ft-lbs (ND8) at the billet interior at 24 °C. This large range of impact toughness both exceeds and falls below the average forged/wrought A508 Grade 4N equivalent (~177 ft-lbs), as reported by Rolls Royce [11], depending on the specimen distance from the canister wall. Similar results are observed compared to the A508 Grade 3 report by EPRI, where an optimum impact toughness was cited as 114 ft-lbs. In either case, the data recorded for billet NC9/ND2/ND6ND8 indicate that, at minimum, the first specimens adjacent to the canister do not meet the forged/wrought equivalent for impact toughness. Specimens located more than two Charpy specimens inboard of the canister (~1 in.) consistently exceed this value.

The impact toughness gradient that develops in PM-HIP A508 Grade 4N has been hypothesized to be due to the presence of oxygen that resides on the surface of the powder particles and is then entrapped in the consolidated material during the HIP process. However, this does not describe why some Charpy specimens exhibit excellent toughness and others are considerably degraded. To further evaluate the location-specific property variation, LECO oxygen measurements from each Charpy specimen tested at 24 °C were performed in triplicate and then plotted in Figure 3. Figure 3 clearly shows that the worst-performing Charpy specimens have the highest oxygen content, and when correlated to the location specific property dependence in Figure 2, it confirms that the oxygen content is not constant through the billet thickness, as suggested by [12]. Instead, oxygen must become mobile during the HIP treatment and create the gradient in oxygen concentration plotted in Figure 4. The severity of the degradation in impact toughness appears to correlate more closely with the pickup in oxygen (relative to starting powder) than absolute oxygen content, as expressed in Figure 3b.

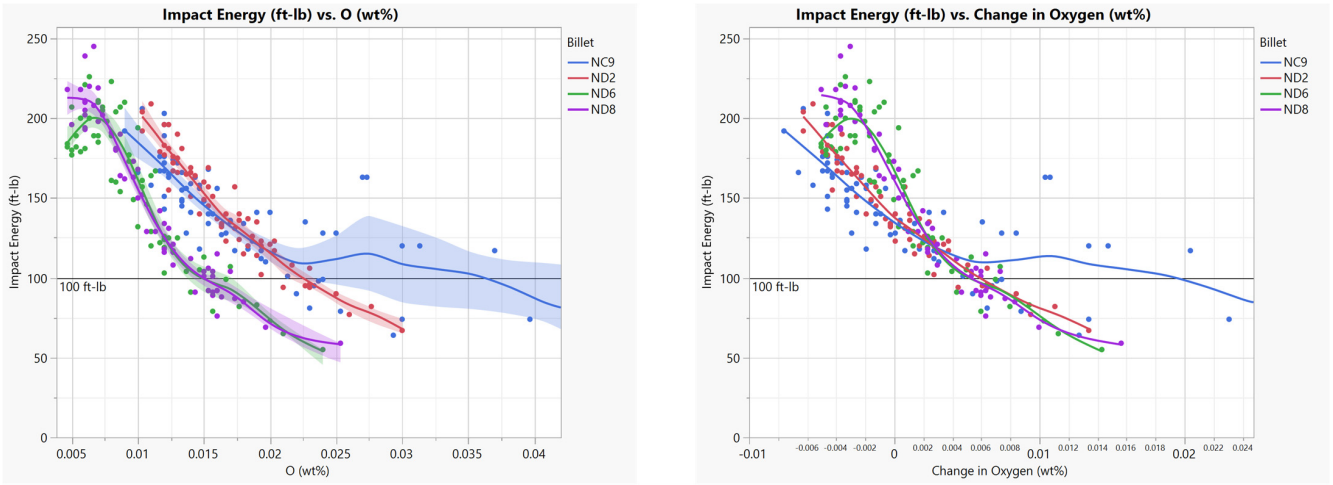

Figure 3. (**a**) Charpy impact toughness trend with oxygen content and (**b**) resulting impact toughness change due to a change in oxygen content relative to original power oxygen content. All data collected at 24 °C.

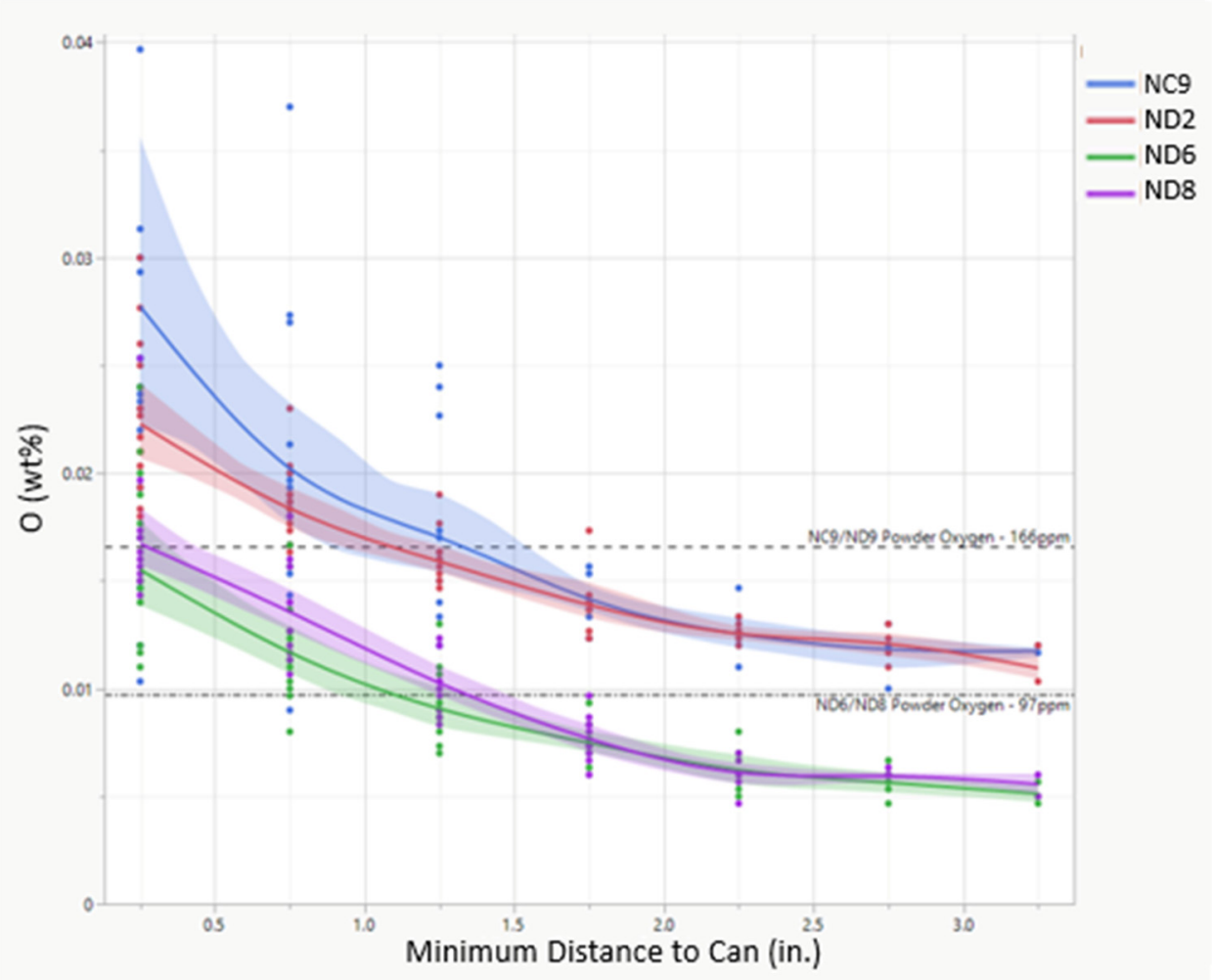

Figure 4. Oxygen content as a function of distance from the canister relative to the starting oxygen content. Dashed lines represent the initial oxygen content for each powder used to fabricate billets NC9/ND2/ND6ND8.

3.2. Development of Oxygen Transport Mechanism

To understand the mechanism resulting in the variation in oxygen content through the billet thickness, the oxygen content for each Charpy specimen was plotted against the nominal oxygen content of the starting powder as supplied by the powder vendor in Figure 4. From Figure 4, it is evident that the oxygen is becoming mobile during the HIP cycle and then redistributing within the billet to result in a gradient in the oxygen content. The direction of oxygen mobility is also clarified in Figure 5, which shows that the oxygen content of the interior Charpy specimens falls below the original powder content and the near-can Charpy specimens exhibit a peak in the oxygen content, meaning that the oxygen must be traveling from the billet interior to the near-can region (i.e., middle out).

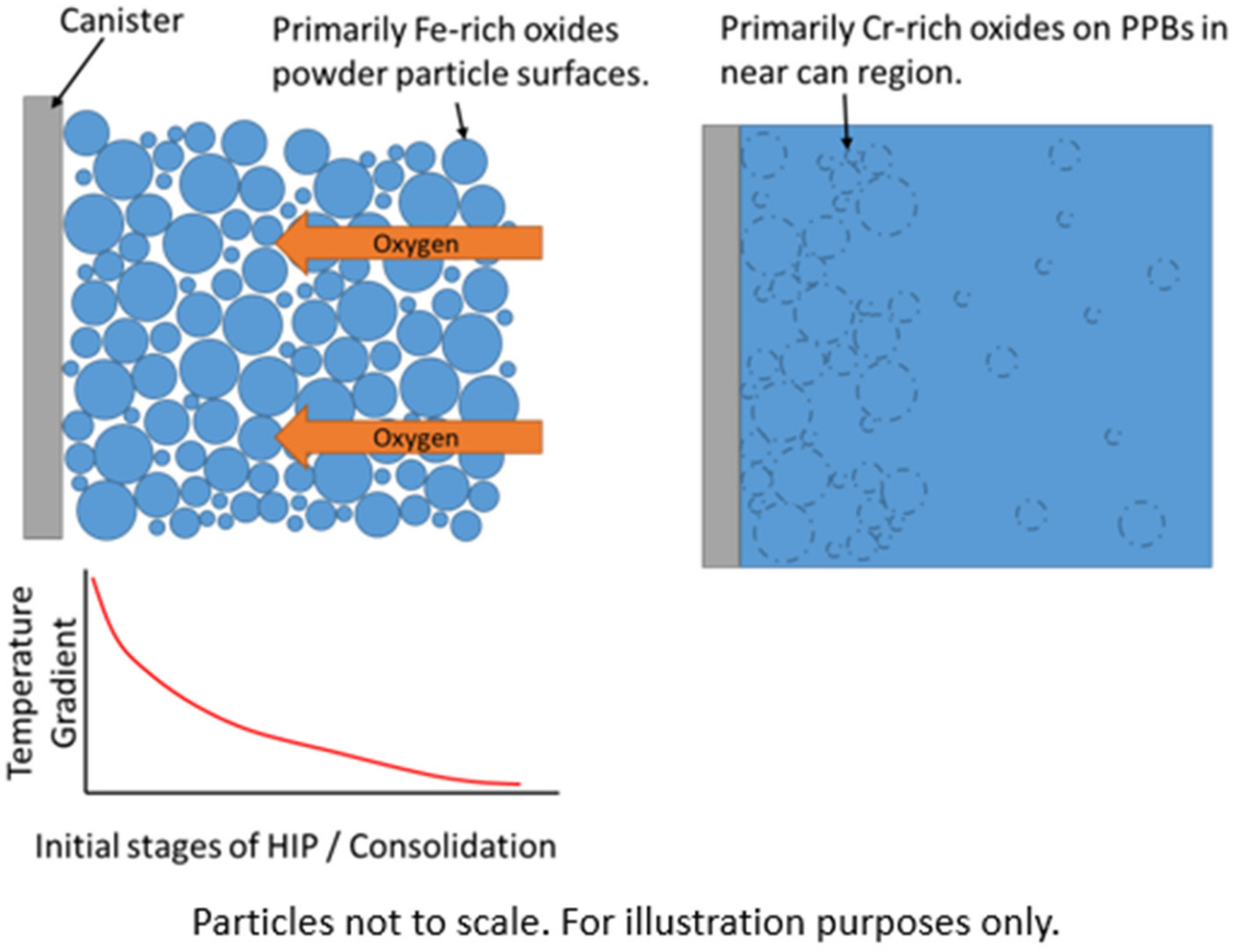

Figure 5. Mechanism describing the migration of oxygen from the interior of the billet to the near-can region during the HIP cycle.

The mechanism to cause such a redistribution in oxygen content is detailed in Figure 5. During the HIP cycle, the powder is not well packed and there is considerable voided space between the powder particles. The lack of particle-to-particle contact increases the difficulty of heat transfer via conduction and results in the outside, or near-can region, of the billet heating up long before the interior. As the temperature increases in the billet, the iron-oxide (Fe_2O_3 or Fe_3O_4 as confirmed in [7]) that resides on the surface of all powder particles begins to off-gas and form carbon-monoxide gas (CO). The decomposition temperature of iron-oxide is not known at high pressures, but the classical Ellingham diagrams suggest that this temperature is near 593 °C. At 593 °C, the powder has yet to consolidate within

the HIP and, thus, for the CO gas, is able to easily pass throughout the billet. Due to the increased temperature (and thus, kinetics) at the near-can region of the billet, the CO gas is driven towards the exterior of the billet, where thermodynamics become favorable for the formation of other stable oxides such as chromium or manganese-oxides. Once these oxides have formed, there is no further driving force for dissolution and the oxides are effectively locked into place at the near-can region and result in an elevated level of oxides at the near-can region.

The presence of chromium or manganese oxides is confirmed via SEM-EDS in Figure 6 and confirms that oxygen is redeposited from billet interiors to the near-can region. The concentration of these oxides would not inherently signal poor mechanical properties, however, as the CO gas can only travel between the powder particles, meaning that the oxygen will likely deposit on the surface of another particle. Upon powder consolidation in the HIP vessel, the newly formed oxide will reside on a prior particle boundary (PPB) that is likely coincident with a prior austenite grain boundary and will inherently drive down the toughness. These chromium and manganese oxides are thermodynamically stable and are locked into place in the near-can regions. The presence of such defects was observed as highly decorated boundaries at the near-can region relative to the billet interior, as shown in Figure 6.

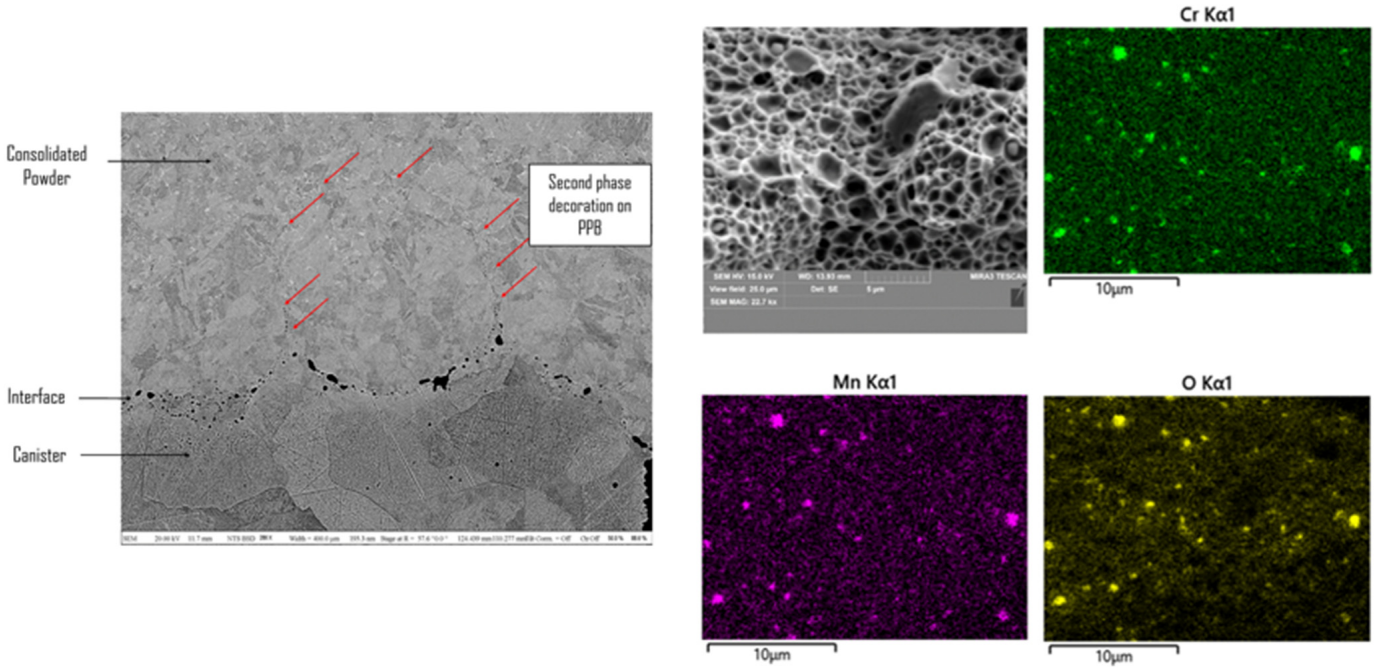

Figure 6. Microstructure of the PM-HIP billet at the canister/billet interface showing heavily decorated boundaries with the appearance of oxides. Corresponding EDS maps of a fracture surface from a specimen extracted near the canister showing a high concentration of Cr-oxides and Mn-oxides.

3.3. Tensile Properties

Room-temperature tensile specimens were tested as a function of specimen distance from the canister, as detailed in Table 3. Similar to the tensile properties observed by Ridgeway et al. [7], the tensile properties of the four billets examined here displayed constant behavior despite the tensile specimen location in the original billet. All tensile specimens passed the existing 24 °C ASTM A508 Grade 4N Class 1 minimum requirements regardless of specimen location. The lack of variation may be due to an elevated level of oxygen through all regions of the billet relative to a forged/wrought product, though it is not fully understood why the variation is observed in impact toughness, but not tensile properties.

Table 3. Average room-temperature tensile properties of each billet relative to the ASTM minimum requirements.

	Temperature	Yield Strength (MPa)	Ultimate Tensile Strength (MPa)	Min Elongation (%)	Min. Reduction in Area (%)
ASTM A508 requirements	24 °C	585	725–895	18	45
NC9	24 °C	667.4 ± 1.4	777.0 ± 3.4	27.7 ± 0.5	76.4 ± 0.5
ND2		647.4 ± 2.1	756.4 ± 3.4	28 ± 0.5	77.1 ± 0.6
ND6		659.8 ± 2.7	779.1 ± 0	28.3 ± 0.5	76.7 ± 0.9
ND8		668.1 ± 2.1	786.0 ± 0	28.1 ± 0.6	76.6 ± 1.2

4. Conclusions

Four billets of PM-HIP A508 Grade 4N were fabricated, heat treated, and tested to reveal the fundamental metallurgical mechanism resulting in the variation in mechanical property performance associated with PM-HIP low-alloy steel. The highlights of this work include the following:

Charpy impact toughness results confirmed the presence of location-specific toughness on all billets despite each billet fabricated under unique processing conditions. The ubiquitous presence of the variation in properties confirms that the mechanism resulting in the variation in impact toughness occurs during HIP and not pre-HIP processing.

The Charpy impact toughness heat maps confirmed that degraded Charpy impact toughness is associated with the material located near the billet/canister interface and tha improved impact toughness is achieved in the material located near the billet interior. Specimens located <~1 in. inboard of the canister routinely fall below the forged wrought equivalent (~177 ft-lbs), while specimens greater than ~1 in. inboard exceed or meet the forged/wrought equivalent impact toughness. The heat maps provide the first detailed analysis of the degradation in properties as they occur through the component thickness.

A chemical analysis conducted through the billet thickness revealed an increase in oxygen content for the material near the original billet/canister interface. This increase in oxygen content was correlated to a reduced impact toughness for the material located up to ~1-inch inboard of the original billet/canister interface. The impact toughness was seen to stabilize in magnitude at 2 in. away from the original billet/canister interface.

A degradation mechanism explaining the oxygen migration during HIP was identified. The mechanism is explained via the dissolution of Fe-oxide on powder particle surfaces that becomes mobile during the HIP cycle and is excited towards the exterior of the billet due to the thermal gradient present through the billet thickness. The mobile oxygen then forms stable chromium and manganese oxides along prior particle boundaries that are coincident with prior austenite grain boundaries near the billet/canister interface. The heavy decoration of boundaries at the near-can region allows for easy crack propagation and results in the reduction in impact toughness relative to the billet interior, which exhibits little to no decoration of boundaries.

Despite the presence of the degraded near-can region, the billet interior exhibited excellent impact toughness (in excess of 200 ft-lbs) and suggests that resolution of the near-can region may result in a PM-HIP A508 Grade 4N that has comparable or better performance than a forged/wrought product. Additionally, with the degradation mechanism now defined, additional research may now be conducted to mitigate the oxygen migration mechanism during the HIP stage, potentially eliminating the variation in impact toughness for PM-HIP A508 Grade 4N, allowing it to be utilized in commercial industry.

Author Contributions: Conceptualization, C.D.R.; methodology, C.D.R. and T.N.; validation, C.D.R. and T.N.; formal analysis, C.D.R.; investigation, C.D.R. and T.N.; resources, C.D.R.; data curation, C.D.R.; writing—original draft preparation, C.D.R.; writing—review and editing, C.D.R. and T.N.; visualization, C.D.R. and J.M.P.; supervision, C.D.R.; project administration, C.D.R. and T.N. All authors have read and agreed to the published version of the manuscript.

Funding: This research received no external funding.

Data Availability Statement: All data will be provided upon request to the corresponding author.

Acknowledgments: The Naval Nuclear Laboratory, including the Knolls Atomic Power Laboratory, is managed and operated for the United States Department of Energy by Fluor Marine Propulsion, LLC, a wholly owned subsidiary of Fluor Corporation.

Conflicts of Interest: The authors declare no conflicts of interest.

References

1. Bassinia, E.; Iannuccia, L.; Lombardia, M.; Biaminoa, S.; Uguesa, D.; Vallilloc, G.; Picqué, B. Net shape HIPping of a Ni-superalloy: A study of the influence of an as leached surface on mechanical properties. *J. Mater. Process. Technol.* **2019**, *271*, 476–487. [CrossRef]
2. Gandy, D. Advanced Technology for Large Scale (ATLAS) Powder Metallurgy-Hot Isostatic Pressing. *EPRI Technol. Assess.* **2016**, 3002007401.
3. *2023 National Defense Strategy of the United States*; Department of Defense: Washington, DC, USA, 2023.
4. *Fact Sheet: White House Calls on Congress to Advance Critical National Security Priorities*; Official Statement from The White House: Washington, DC, USA, 2023.
5. *Navy Force Structure and Shipbuilding Plans: Background and Issues for Congress. Congressional Research Service*; RL32665; Materials Research Forum, LLC.: Millersville, PA, USA, 2022.
6. *Report to Congress on the Annual Long-Range Plan for Construction of Naval Vessels for Fiscal Year 2023*; Prepared by Office of the Chief of Naval Operations. Deputy Chief of Naval Operations for Warfighting Requirements and Capabilities—OPNAV N9. Approved for Release by: Office of Secretary of the Navy; 2022. Available online: https://media.defense.gov/2022/Apr/20/2002980535/-1/-1/0/PB23%20SHIPBUILDING%20PLAN%2018%20APR%202022%20FINAL.PDF (accessed on 20 June 2024).
7. Ridgeway, C.; Nolan, T. *Powder Metallurgy HIP for Naval Nuclear Applications—Trends in Process and Property Development*; HIP'22. Materials Research Proceedings; Hot Isostatic Pressing; Materials Research Forum, LLC.: Millersville, PA, USA, 2023; Volume 38, pp. 41–47.
8. Gandy, D.; Tate, S.; Albert, M. *Advanced Nuclear Technology: Code Development of PM-HIP Alloy A508–Progress Report*; Technical Update, Deliverable 3002018274; 2021. Available online: https://www.mrforum.com/wp-content/uploads/open_access/9781644902837/7.pdf (accessed on 20 June 2024).
9. Sulley, J.; Hookham, I.; Burdett, B.; Bridger, K. Introduction of Hot Isostatically Pressed, Reactor Coolant System Components in PWR Plant. In Proceedings of the 18th International Conference on Nuclear Engineering ICONE18, Xi'an, China, 17–21 May 2010.
10. Stewart, D.; Sulley, J.; Warner, T.; Wallace, P.; Jones, G.; Thatcher, D. Mechanical Properties and Metallurgical Examination Results for a Batch of Powder Metallurgy—Hot Isostatically Pressed Low Alloy Steel Grade 508 4N Alloy. In Proceedings of the ASME 2022 Pressure Vessels & Piping Conference—PVP2022, Las Vegas, NV, USA, 17–22 July 2022.
11. Stewart, D.; Sulley, J.; Thatcher, D. Mechanical Properties and Metallurgical Examination Results for Batches of Powder Metallurgy—Hot Isostatically Pressed Low Alloy Steel Grade 508 4N Alloy. In Proceedings of the ICAPP, Busan, Republic of Korea, 30 April–3 May 2023. Gyeongju, Korea Paper 2023324.
12. Irukuvaraghula, S.; Hassanin, H.; Cayron, C.; Aristizabal, M.; Attallah, M.; Preuss, M. Effect of Powder Characteristics and Oxygen Content on Modifications to the Microstructural Topology during Hot Isostatic Pressing of an Austenitic Steel. *Acta Mater.* **2019**, *172*, 6–17. [CrossRef]